PHYSICAL REVIEW B **74**, 035309 (2006)

Structure of the interface between ultrathin SiO_2 films and 4*H*-SiC(0001)

Mark Schürmann,* Stefan Dreiner, Ulf Berges, and Carsten Westphal
Experimentelle Physik 1, Universität Dortmund, Otto-Hahn-Strasse 4, 44221 Dortmund, Germany
(Received 2 March 2006; published 12 July 2006)

The interface between ultrathin SiO_2 films and 4*H*-SiC(0001) has been studied by x-ray photoelectron spectroscopy (XPS) and photoelectron diffraction. The investigation was performed for two different films. An ordered silicate layer showed a clear $(\sqrt{3}\times\sqrt{3})R30°$ reconstruction, whereas a second film showed no long-range order. The comparison of the photoelectron diffraction data from these two films reveals that the local atomic environments of the Si atoms at the interface are very similar in both films. Further, a comparison of the experimental data with simulation calculations within a comprehensive *R*-factor analysis shows that also the local environments around near-interface Si atoms inside the SiO_2 film are similar, but some modifications to the model are necessary. The use of the cluster radius as a fitting parameter in the simulation allowed to estimate the size of locally ordered regions in the film without long-range order to be about 4.5 to 5.0 Å. It turns out that the transition from SiC to SiO_2 is abrupt and therefore the occurrence of defects in the SiO_2 film near the interface is probable. These defects may be oxygen vacancies, oxygen dangling bonds or silicon interstitials.

DOI: 10.1103/PhysRevB.74.035309 PACS number(s): 61.14.Qp, 79.60.Dp, 81.65.Mq

I. INTRODUCTION

Silicon carbide is a promising semiconductor material for the fabrication of microelectronic devices. Due to its wide band gap, it is suitable for applications related to high power, high frequencies, and high temperatures. The recent progress in the growth of high quality SiC wafers[1,2] increases the possibilities of SiC in device applications. For an application in the metal-oxide-semiconductor (MOS) technology it is beneficial that SiC can be, as Si, thermally oxidized to form an insulating SiO_2 film at the surface. However, in contrast to silicon, the SiO_2/SiC interface is not ideal in the respect that, due to the high concentration of defects, it exhibits a high density of states at the interface which reduces the quality of SiC based devices.[3–5] Up to now, the nature of these interface defects is unclear. There are indications that they can be attributed to carbon or silicon dangling bond at the interface,[6] carbon interstitials in SiC or at the interface,[7–9] silicon interstitials in the oxide,[10] carbon contaminations in the silicon oxide film,[4,11] or silicon suboxides which are formed at the interface due to geometric constraints of the SiC surfaces.[12] To shed further light on the origin of the defects, a detailed understanding of the atomic structure of the interface is necessary.

In general, thermal oxidation of SiC surfaces leads to SiO_2 films which show no long-range order. In contrast, Bernhardt *et al.* discovered that ordered silicate layers on both SiC(0001) and SiC(000$\bar{1}$) surfaces are formed if the surface is treated with hydrogen plasma or if it is etched in hydrogen flow[13] with the hydrogen containing oxygen contaminations in both cases. Different ordered silicate layers have been investigated experimentally and theoretically and structure models were proposed.[13–15] While these silicate layers exhibit sharp interfaces and perfectly crystalline oxide films, no successful growth of thicker silicon oxide films on top of these layers has been reported. However, it is interesting to note, that photoemission studies of such ordered silicate layers[16] show the same three components as were also observed in studies of nonordered thermally grown SiO_2 films.[17] This observation raises the question about the difference in the local atomic structure at the SiO_2/SiC interface for the two different films. Knowledge about these differences represents a key to a better understanding of the nonideal nature of the SiO_2/SiC interface and thus the possible origins of the high density of interfacial defects.

In this paper we report on angle-scanned x-ray photoelectron diffraction (XPD) measurements on the SiO_2/SiC interface. The method applied proved to be appropriate for interface investigations of crystalline silicon covered by amorphous silicon oxide films.[18,19] The short inelastic mean free path of the outgoing photoelectrons provides a surface sensitive tool to investigate the local structure of internal interfaces around the emitting atoms. XPD allows one to collect information from several layers beneath the surface and due to its chemical sensitivity it is a unique tool to distinguish between different emitter types located in different local environments. Therefore photoelectron diffraction is one of very few techniques which allow experimental access to the atomic structure of buried interfaces. We apply XPD here to investigate both an ordered silicate layer and an ultrathin silicon oxide layer without any long-range order. The results were compared and simulations were carried out to explain the observed differences in the experimental diffraction patterns and to get a better understanding of the local atomic structure at the SiO_2/SiC interface for nonordered thermally grown films.

II. EXPERIMENTAL

All samples were cut from a single-crystalline, Al-doped 4*H*-SiC(0001) wafer which was 8° off-axis oriented. The samples were cleaned in UHV by heating them in a Si-flux provided by an electron beam evaporator. For all experiments a clean $(\sqrt{3}\times\sqrt{3})R30°$-reconstructed surface was used as a starting point, as routinely checked by low energy electron diffraction (LEED). The sample was exposed to 1

 ©2006 The American Physical Society

$\times 10^{-4}$ mbar partial pressure of oxygen for 30 minutes at a temperature of 800 °C leading to ultrathin SiO_2 films. In LEED sharp 1×1 spots of the substrate were displayed, indicating that the ultrathin layer of covering silicon oxide exhibited no long-range order. Ordered silicate films could also be prepared in the UHV chamber. Therefore very silicon rich surfaces were exposed to oxygen contaminated by water with the samples held at temperatures of about 900 °C. In this case a $(\sqrt{3}\times\sqrt{3})R30°$ pattern was observed by LEED. For both films no carbon contaminations were present within the detection limit of x-ray photoelectron spectroscopy (XPS).

The photoemission spectra were recorded at the U41-PGM beamline at BESSY II in Berlin. All data were recorded with a photon energy of $h\nu=180$ eV. At this energy a very high photon flux is provided by the beamline, and the photoemission cross section for the Si $2p$ signal is large. Further, at this excitation energy the resulting photoelectrons have a kinetic energy of approximately 80 eV and therefore the experimental data are very surface sensitive. Due to the short inelastic mean free path of the photoelectrons the use of small model clusters ($\lesssim$250 atoms) in the photoelectron diffraction simulations became possible. The overall energy resolution (photons and electron analyzer) was set to 100 meV which was sufficient to separate the spectral components in the Si $2p$ spectra. Photoelectron diffraction data were recorded by rotating the sample with increments of 2° both around azimuthal $(0°<\Phi<360°)$ and polar angles $(0°<\Theta<80°)$ and measuring the Si $2p$ intensity under each angle.[18] The simulations were performed using the program MSPHD.[20] This program is especially suitable for the computation of photoelectron diffraction effects at low kinetic energies due to the use of a complex potential and it was already successfully applied to photoelectron diffraction studies.[19,21]

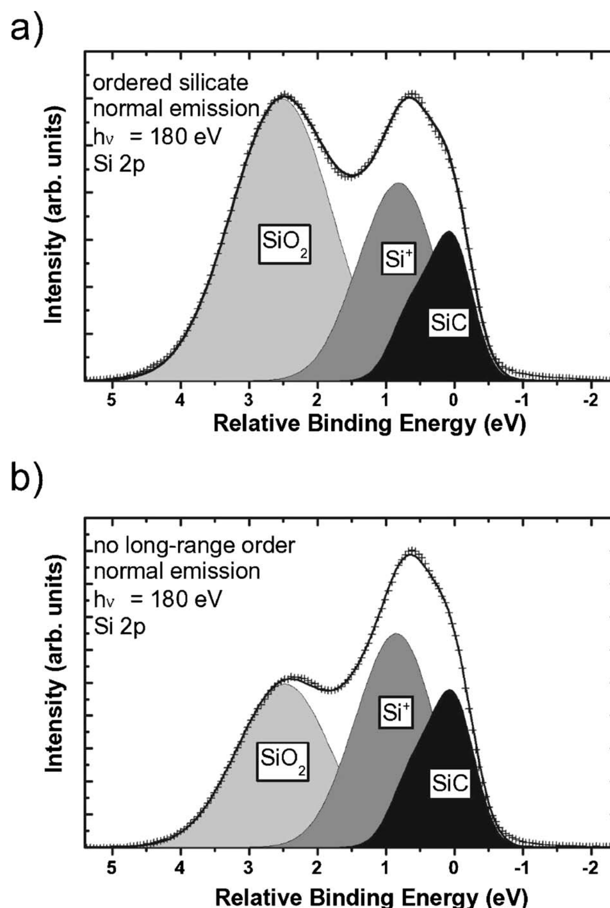

FIG. 1. Si $2p$ core-level spectra of a $4H$-SiC(0001) sample with an ordered silicate layer (a) and a sample covered by a silicon oxide film which showed no long-range order (b). Both spectra were recorded in normal emission with a photon energy of 180 eV. Each line consists of the spin-orbit split Si $2p_{1/2}$ and Si $2p_{3/2}$ components.

III. RESULTS AND DISCUSSION

Figure 1 shows photoemission spectra of the Si $2p$ line (consisting of the spin-orbit split Si $2p_{1/2}$ and Si $2p_{3/2}$ lines) for the ordered silicate layer (a) and the silicon oxide film without long-range order (b). Both spectra can be decomposed into three components. The "SiC" component originates from Si emitters located within the SiC substrate which have four bonds to carbon atoms. A "SiO_2" component is shifted by 2.3 eV to a higher binding energy. It can be ascribed to silicon emitters which have four bonds to oxygen atoms. Finally, the "Si^{+}" component is shifted by 0.64 eV [Fig. 1(a)] or by 0.69 eV [Fig. 1(b)] to a higher binding energy. The emitter atoms are located at the interface with one bond to oxygen and three bonds to carbon atoms. It is noteworthy, that unlike for the SiO_2/Si interface[22] no further intermediate oxidation states than the Si^{+} component are displayed in the XPS spectra. This was observed by Sieber *et al.* in their photoemission study of ordered silicate layers on SiC(0001) (Ref. 16) and was also found by photoemission studies of nonordered SiO_2 films on hexagonal SiC surfaces (e.g., Refs. 17 and 23). Interfacial components corresponding to the intermediate oxidation states of the SiO_2/Si interface were found only for the oxidation of Si-rich 3×3-reconstructed $4H$-SiC and $6H$-SiC surfaces at low oxygen pressures and low temperatures ($\leq$650 °C).[24] Also, different and/or additional chemical shifted Si $2p$ components were detected in photoemission studies of SiO_2 films on differently oriented polar and nonpolar $4H$-SiC samples.[25,26] The latter observation indicates that the emitters contributing to the Si^{+} component are related to the SiO_2/SiC(0001) interface and that this interface is different for differently oriented samples.

The spectrum of the ordered silicate layer [Fig. 1(a)] exhibits a larger SiO_2 component than the spectrum of the film without long-range order [Fig. 1(b)]. This indicates a thicker oxide film for the silicate layer or an only partially covered surface of the nonordered film. The thickness of both films can be estimated by polar-angle dependent XPS. Figure 2 shows the intensity ratio of the SiO_2 component to the sum of Si^{+} and SiC components plotted against the emission angle. The fit in Fig. 2(a) is based on a model which includes the damping of the SiC- and Si^{+}-photoemission signals by a closed SiO_2 overlayer covering the whole surface. Assuming an effective attenuation length of the electrons of 3.5 Å, an

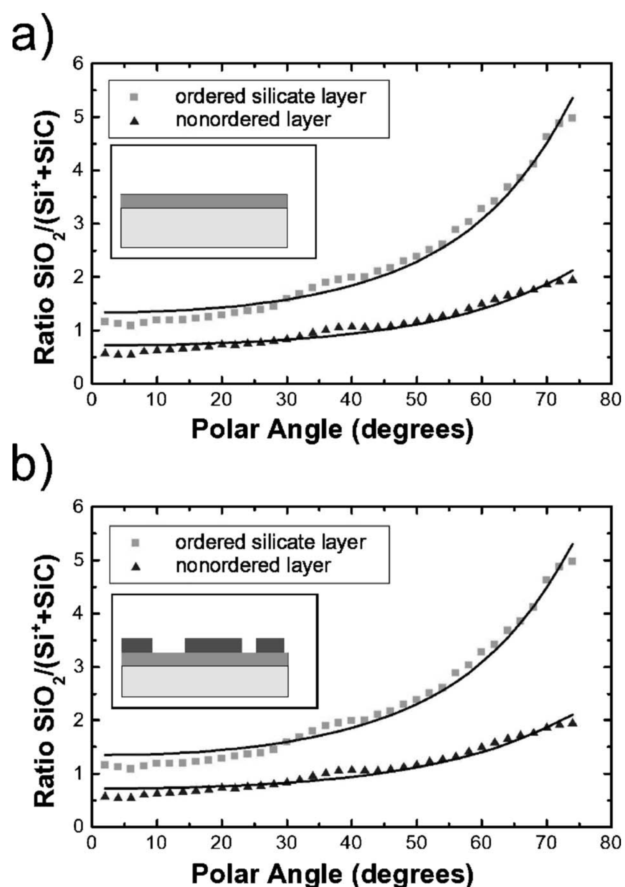

FIG. 2. Polar-angle dependence of the XPS signal. Symbols denote the experimental data [ratio $SiO_2/(Si^{+}+SiC)$], solid lines represent the result of a fit to the data. Polar angles are given with respect to the surface normal. The fits were based on a model of an exponential damping in a closed SiO_2 film covering the whole surface (a) and on a complete coverage of the surface with O atoms but only a partial coverage with SiO_2 (b).

inner potential of 15 eV and a density ratio of 0.75 of Si emitter atoms in SiO_2 to Si emitters in SiC, the only remaining free parameter is the thickness of the silicon oxide film. With this model, a thickness of the ordered silicate layer of 3.59 Å is obtained, which fits well with the structure model for this film proposed by Bernhardt *et al.*[13] For the nonordered film a thickness of 2.31 Å is obtained by the fit. The value of 2.31 Å appears rather low considering that the Si-O bond length is about 1.6 Å and that the SiO_2 emitters have four bonds to oxygen atoms. This finding suggests, that SiO_2 is only partially covering the surface of this sample. Therefore, the model was modified to take the partial coverage of the surface into account. The result of the fitting with this modified model is shown in Fig. 2(b). The modified model assumes that the Si layer at the interface is completely covered by oxygen. This assumption is confirmed by the photoelectron diffraction results presented later. On top of this oxygen layer of 1.6 Å thickness (corresponding to the Si-O bond length) a silicon oxide film is assumed which partially covers the surface. Within this model the thickness of the SiO_2 film and the coverage are left as free parameters. For the ordered film a thickness of 3.76 Å and a coverage of 96% are determined by the fit with this model. Both values agree well with the assumption of an ordered silicate layer covering the whole surface. In the case of the nonordered film a thickness of 3.55 Å and a coverage of 68% resulted from the fit. This indicates, that the thickness of the nonordered film is similar to the thickness of the ordered silicate, and that the silicon oxide covers only a fraction of the surface.

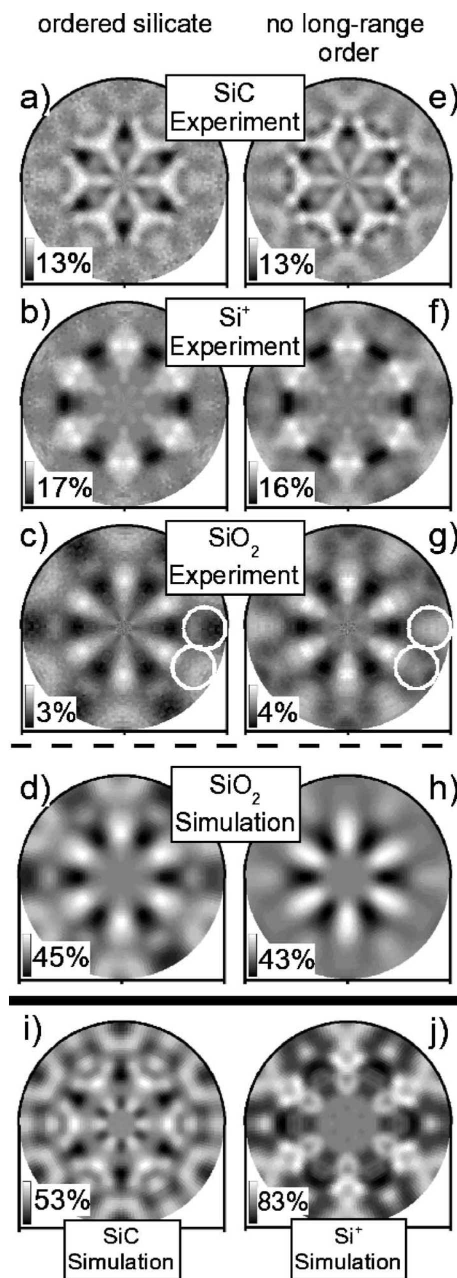

FIG. 3. Experimental and simulated photoelectron diffraction patterns of the Si 2p emission line for an ordered silicate film [(a)–(d)] and a silicon oxide film without long-range order [(e)–(h),(i),(j)]. The photon energy was 180 eV and the angular resolution of the detector about ±3°.

Figure 3 shows the photoelectron diffraction patterns corresponding to the three components displayed in Fig. 1 for both films. The patterns are plotted as the anisotropy function

$$\chi(\Theta,\Phi) = \frac{I(\Theta,\Phi) - I_0(\Theta)}{I_0(\Theta)}$$

in order to be independent from experimental asymmetries and differential cross-section effects, where $I(\Theta,\Phi)$ denotes the intensity measured at the angle (Θ,Φ) and $I_0(\Theta)$ the mean intensity in the respective polar angle. The χ function is displayed in a linear greyscale, with the maximum anisotropy $(\max[\chi(\Theta,\Phi)]-\min[\chi(\Theta,\Phi)])$ displayed in the lower left-hand corner each. The patterns of the ordered silicate film and the patterns of the film without long-range order are shown in the left-hand and right-hand column, respectively. All three components (SiC, Si^+, SiO_2) show their own individual intensity distribution for both films, indicating different local atomic environments for each emitter type.

The patterns of the SiC emitter [Figs. 3(a) and 3(e)] are nearly identical for both films. This was expected since photoelectron diffraction is very sensitive to the atom positions in the nearest environment around the emitter atoms and in both samples Si atoms of the SiC bulk are located in identical atomic environments. The same can be observed for the Si^+ diffraction patterns measured at both samples [Figs. 3(b) and 3(f)]. Again both patterns show the same features. This means that in spite of the differences between the two SiO_2 films the local atomic environment of the Si atoms at the interface is very similar in both films. This leads to the conclusion that the main structural differences between the two films are to be found inside the silicon oxide film. Indeed, large differences between these two films can be seen in their SiO_2 diffraction patterns [Figs. 3(c) and 3(g)]. These patterns show very different features. Especially at high polar angles different intensity distributions (marked with white circles) are displayed. Therefore the Si atoms in the near interface region of the two SiO_2 films are situated in different local atomic environments.

In order to obtain structural information from the experimental photoelectron diffraction patterns, simulation calculations were performed. The results were compared to the experimental data within an R-factor analysis with the R-factor defined as $R=\frac{\Sigma(\chi_S-\chi_E)^2}{\Sigma(\chi_S^2+\chi_E^2)}$. The experimental and simulated anisotropy functions χ_E and χ_S are mainly a measure for the strength of the diffraction effects. Different models were tested and within each model a number of parameters were varied. A search algorithm was applied in order to find the global minimum of the R-factor in the parameter space. This algorithm[27] was originally used in tensor-LEED investigations and was adapted to the analysis of photoelectron diffraction data. The model for the ordered silicate layer proposed by Bernhardt and co-workers[13] was chosen as a starting point for the simulations (cf. Fig. 4). This approach suggested itself, because the ordered film was supposed to be a silicate layer with the same structure as the films prepared by Bernhardt *et al.*, and because for the nonordered film two of the three experimental diffraction patterns are very similar to the respective patterns measured for the ordered film. In the simulations, spherical clusters centered around the respective emitter atom were used. The radius of the cluster

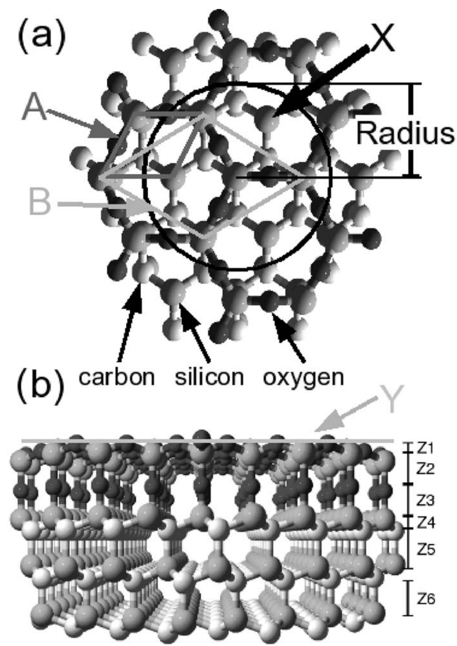

FIG. 4. Structure model for the ordered silicate layer from Ref. 13, top (a) and side (b) view. Carbon is depicted as light gray, silicon as gray, and oxygen as dark gray. The rhombs A and B mark the (1×1) and $(\sqrt{3}\times\sqrt{3})R30°$ unit cells of the ideal substrate and the ordered film, respectively. The atom at X is a silicon atom at the interface which can have one dangling bond in the model. Oxygen atoms at Y must be omitted in the model structure for the nonordered film. Vertical distances from $Z1$ to $Z6$ and the radius were used as parameters in simulations.

and the vertical distances from $Z1$ to $Z6$ were used as fitting parameters in the R-factor analysis.

The experimental SiO_2 pattern [Fig. 3(c)] could be reproduced by simulations based on the existing model for the ordered silicate layer. Figure 3(d) depicts the simulated pattern with the lowest R-factor ($R=0.09$) in the R-factor analysis which bears the closest resemblance to the experimental pattern. The R-factor was slightly improved from $R=0.11$ to $R=0.09$ by saturating the remaining dangling bonds of the silicon interface atoms [X in Fig. 4(a)] with oxygen atoms in the model. The agreement indicates, that the ordered film investigated here and the silicate layer described by Bernhardt *et al.* had the same structure. In contrast to the pattern of the ordered film [Fig. 3(c)] the pattern of the nonordered SiO_2 layer [Fig. 3(g)] shows a very different intensity distribution. In this case it was not possible to reproduce the pattern with simulations based on the model of the ordered silicate layer. Modifications to the structure model were necessary to achieve accordance between simulated and experimental data. In the modified model all silicon atoms at the interface [including X atoms in Fig. 4(a)] must have one bond to an oxygen atom in the SiO_2 film. This reduced the R-factor by a factor of 2. Furthermore, the top layer of oxygen atoms [cf. Y atoms in Fig. 4(b)] must be removed from the structure model. The latter fact is an indication, that no ordered structure was located above the SiO_2 emitter atoms in the nonordered film. In particular, the oxygen connections between the Si atoms in the ordered silicate structure which

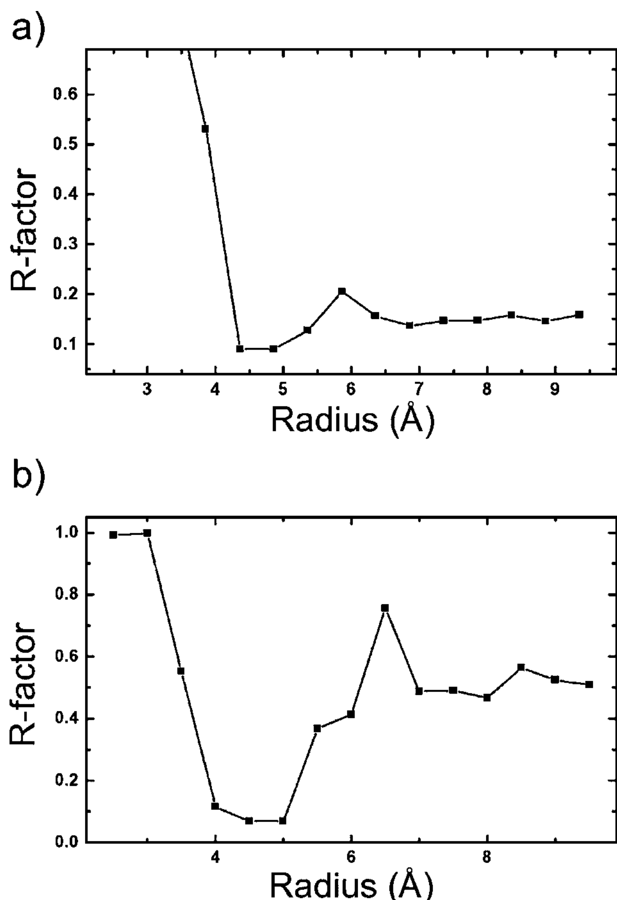

FIG. 5. Dependence of the *R*-factor on the radius of the model cluster for an ordered silicate layer (a) and for a film without long-range order (b).

are responsible for the honeycomblike shape, are not present in the modified model. Apparently, these oxygen bonds are randomly directed in the nonordered film and therefore these oxygen atoms are not contributing as scatterers to the photoelectron diffraction signal. With these two changes in the structure model the *R*-factor analysis resulted in a very good agreement between experimental [Fig. 3(g)] and simulated [Fig. 3(h)] pattern with an *R*-factor of 0.07. Also, the photoelectron diffraction patterns of the SiC and the Si^+ components were calculated with this model. In both cases the simulated patterns were compared with the experimental patterns of the nonordered film within an *R*-factor analysis. The simulated patterns for the SiC and the Si^+ components are shown in Fig. 3(i) and Fig. 3(j) with corresponding *R* factors of $R=0.17$ and $R=0.11$, respectively.

In all *R*-factor analyses, the radius of the model cluster was used as a fitting parameter. The dependence of the *R*-factor on the cluster radius contains information about the size of ordered regions on the surface. Figure 5(a) displays the *R*-factor as a function of the radius of the model cluster for the ordered silicate film. The *R*-factor curve has it's minimum at a value of 4.5 to 5.0 Å for the cluster radius. For lower values the *R*-factor increases steeply due to missing scatterer atoms in the simulation. For a cluster radius above ~5 Å only a gentle increase of the *R*-factor can be observed. For an experiment under ideal conditions with a perfectly ordered silicate film, without any steps and defects, and with a perfect account for inelastic scattering within the simulations, no increase for larger radii would be expected. The observed gentle increase of the *R*-factor in Fig. 5(a) can result from surface steps and from defects in the silicate film. The *R*-factor curve for the nonordered film [Fig. 5(b)] looks different. Again, a minimum of the *R*-factor is displayed for a cluster radius of 4.5 to 5.0 Å and a steep increase for smaller radii is observed. However, in this case also for larger cluster radii the *R*-factor increases rapidly from 0.07 to 0.4 if the radius is changed to values larger than 5.5 Å. Therefore the radius of the cluster can be interpreted as a measure of the size of ordered regions around the emitting atoms in the film. In smaller clusters important scatterers are missing and it is not possible to reproduce the experimental diffraction patterns. In larger clusters, additional scatterers contribute to the simulated pattern such that the agreement with the experimental data is strongly reduced.

These findings from the photoelectron diffraction analysis match well to the XPS data and explain, why the same three components appear in spectra of the ordered silicate layer and in spectra of nonordered silicon oxide films. In both types of oxide films, both the Si^+ emitters at the interface and the SiO_2 emitters near the interface are located in very similar local atomic environments. The silicon interface atoms which, according to the model for the ordered silicate, possibly carry a dangling bond (X atoms in Fig. 4) are saturated by oxygen atoms in the nonordered film. However, as the simulations showed, the same could not be excluded for the case of the ordered film investigated in this work. Therefore, the only structural difference between these two films is the smaller size of ordered regions in the nonordered film and, correlated to that, the absence of oriented bonds of the near-interface Si atoms to oxygen atoms (Y atoms in Fig. 4). This result gives a hint to explain the high density of defects at the $SiO_2/4H$-SiC(0001) interface for nonordered silicon oxide films. The transition from the SiC substrate to the SiO_2 film appears to be abrupt because no intermediate oxidation states are observed in the Si 2*p* XPS spectra (Fig. 1) and because no indication was found for C-O bonds in the C1*s* spectra (not shown). The local environment of near-interface Si atoms in the nonordered oxide films is the same as of Si atoms in the ordered silicate layer. However, no long-range order exists in the SiO_2 film and the oxygen bonds of the near-interface Si atoms show no preferential orientation relative to the SiC lattice. Therefore one origin of defects might be related to the way in which the connections between the near-interface Si atoms inside the oxide film are made and in which the remaining bonds of O atoms near the interface are saturated. Some possibilities suggest themselves: Si interstitials, oxygen vacancies, oxygen dangling bonds in the SiO_2 film near the interface, or a combination of these three. Due to their possibly low concentrations and the limitations of the methods applied, none of these defects could be observed directly. However, some of them fit with recent experimental and theoretical results: Indications for oxygen dangling bonds were found by Maekawa *et al.* by positron annihilation spectroscopy.[28] A recent theoretical study[10] suggested Si interstitials near the interface inside the SiO_2 film as the origin of near interface traps.

IV. SUMMARY

In conclusion we report on a photoelectron diffraction investigation of oxidized 4*H*-SiC(0001). The structural differences between two different oxide films were studied. In particular, the atomic structure at the interface of an ordered silicate film and an ultrathin silicon oxide film without long-range order were compared. It was possible to get experimental access to the local atomic structure at the interface between 4*H*-SiC(0001) and thermally grown, nonordered SiO_2 films. We show, that the local atomic environment of the silicon atoms at the interface is very similar in both films. Differences appear only in the first oxide layers directly above the interface. For the film without long-range order, each silicon interface atom is bonded to an oxygen atom. Silicon atoms in the bottom layer of the oxide are positioned in a similar local atomic environment as in the ordered silicate layer, but the size of ordered regions around them is only around 4.5 Å. No ordered structure can be detected above these Si atoms in the SiO_2 film, and they form three bonds to oxygen which are not oriented with respect to the underlying substrate. In combination with the XPS results these findings suggest, that important sources of defects could be located at the SiO_2 side of the interface in the form of Si interstitials, oxygen vacancies, or oxygen dangling bonds.

It is proposed, that the knowledge about the interface structure between ultrathin SiO_2 films and hexagonal SiC gained from this work is transferable to interfaces with SiO_2 layers which are thicker than the investigated films: Apparently the transition from SiC to SiO_2 is abrupt and therefore it should not depend on the thickness of the oxide film. This assumption is seconded by XPS investigations by Virojanadara and Johansson[29] who observe no additional component in their spectra when the SiO_2 thickness is increased. The knowledge about the atomic structure at the interface, which was gained from this study, contributes to a better understanding of this technologically important interface and maybe inspire further experimental or theoretical investigations. Also, these findings about the local atomic structure at the interface could be relevant in the context of the question why it is possible to improve the interface quality, for example, by heating the sample in H_2, NO or N_2O (Ref. 30) environments. Further this study indicates that, due to it's element specificity, photoelectron diffraction might be a promising method to investigate the mode of action of nitrogen atoms at the interface.

ACKNOWLEDGMENTS

The authors thank the BESSY II team, especially Ch. Jung, for the kind support during the measurements. This work was partially supported by the German Research Foundation (DFG) under Contract No. WE1649/7-1.

*Electronic address: mark.schuermann@uni-dortmund.de

[1] R. Madar, Nature (London) **430**, 974 (2004).
[2] D. Nakamura, I. Gunjishima, S. Yamaguchi, T. Ito, A. Okamoto, H. Kondo, S. Onda, and K. Takatori, Nature (London) **430**, 1009 (2004).
[3] J. Tan, M. K. Das, J. A. Cooper, Jr., and M. R. Melloch, Appl. Phys. Lett. **70**, 2280 (1997).
[4] V. V. Afanasev, M. Bassler, G. Pensl, and M. Schulz, Phys. Status Solidi A **162**, 321 (1997).
[5] N. S. Saks, S. S. Mani, and A. K. Agarwal, Appl. Phys. Lett. **76**, 2250 (2000).
[6] J. L. Cantin, H. J. von Bardeleben, Y. Shishkin, Y. Ke, R. P. Devaty, and W. J. Choyke, Phys. Rev. Lett. **92**, 015502 (2004).
[7] M. Di Ventra and S. T. Pantelides, Phys. Rev. Lett. **83**, 1624 (1999).
[8] K. C. Chang, N. T. Nuhfer, L. M. Porter, and Q. Wahab, Appl. Phys. Lett. **77**, 2186 (2000).
[9] J. M. Knaup, P. Deak, T. Frauenheim, A. Gali, Z. Hajnal, and W. J. Choyke, Phys. Rev. B **71**, 235321 (2005).
[10] J. M. Knaup, P. Deak, T. Frauenheim, A. Gali, Z. Hajnal, and W. J. Choyke, Phys. Rev. B **72**, 115323 (2005).
[11] S. Wang, M. Di Ventra, S. G. Kim, and S. T. Pantelides, Phys. Rev. Lett. **86**, 5946 (2001).
[12] R. Buczko, S. J. Pennycook, and S. T. Pantelides, Phys. Rev. Lett. **84**, 943 (2001).
[13] J. Bernhardt, J. Schardt, U. Starke, and K. Heinz, Appl. Phys. Lett. **74**, 1084 (1999).
[14] Y. Hoshino, R. Fukuyama, and Y. Kido, Phys. Rev. B **70**, 165303 (2004).
[15] W. Lu, P. Krüger, and J. Pollmann, Phys. Rev. B **61**, 13737 (2000).
[16] N. Sieber, M. Hollering, J. Ristein, and L. Ley, Mater. Sci. Forum **338-342**, 391 (2000).
[17] C. Virojanadara and L. I. Johansson, Surf. Sci. Lett. **472**, L145 (2001).
[18] S. Dreiner, M. Schürmann, C. Westphal, and H. Zacharias, Phys. Rev. Lett. **86**, 4068 (2001).
[19] S. Dreiner, M. Schürmann, and C. Westphal, Phys. Rev. Lett. **93**, 126101 (2004).
[20] R. Gunnella, F. Solal, D. Sebilleau, and C. R. L. Natoli, Comput. Phys. Commun. **132**, 251 (2000).
[21] R. Gunnella, E. L. Bullock, L. Patthey, C. R. Natoli, T. Abukawa, S. Kono, and L. S. O. Johansson, Phys. Rev. B **57**, 14739 (1998).
[22] F. J. Himpsel, F. R. McFeely, A. Taleb-Ibrahimi, J. A. Yarmoff, and G. Hollinger, Phys. Rev. B **38**, 6084 (1988).
[23] D. Schmeißer, D. R. Batchelor, R. P. Mikalo, P. Hoffmann, and A. Lloyd-Spetz, Appl. Surf. Sci. **184**, 340 (2001).
[24] F. Amy, P. Soukiassian, Y. K. Hwu, and C. Brylinski, Phys. Rev. B **65**, 165323 (2002).
[25] C. Virojanadara and L. I. Johansson, Phys. Rev. B **68**, 125314 (2003).
[26] C. Virojanadara and L. I. Johansson, Phys. Rev. B **71**, 195335 (2005).
[27] M. Kottcke and K. Heinz, Surf. Sci. **376**, 352 (1997).
[28] M. Maekawa, A. Kawasuso, Z. Q. Chen, M. Yoshikawa, R. Suzuki, and T. Ohdaira, Appl. Surf. Sci. **244**, 322 (2005).
[29] C. Virojanadara and L. I. Johansson, Surf. Sci. **505**, 358 (2002).
[30] S. Dhar, S. R. Wang, J. R. Williams, S. T. Pantelides, and L. C. Feldman, MRS Bull. **30**, 288 (2005).